Scaling of the anomalous Hall effect in perpendicularly magnetized epitaxial films of the ferrimagnet $NiCo_2O_4$

Daisuke Kan,* Lingling Xie, and Yuichi Shimakawa
Institute for Chemical Research, Kyoto University, Uji, Kyoto 611-0011, Japan

(Received 19 July 2021; accepted 28 September 2021; published 11 October 2021)

We investigate the anomalous Hall effect in perpendicularly magnetized ferrimagnet $NiCo_2O_4$ epitaxial films 3 to 30 nm thick. We find that the anomalous Hall conductivity σ_{AHE} has complex relations with the longitudinal electrical conductivity σ_{xx}. When the σ_{xx} is relatively large (larger than $10^3\,\Omega^{-1}\,cm^{-1}$), the σ_{AHE} is almost independent of the σ_{xx}, but scales with the magnetization. This unique scaling behavior of σ_{AHE} indicates that the anomalous Hall effect is of intrinsic origin dominated by the Berry curvature of occupied electronic states. On the other hand, when the σ_{xx} is lowered, the scaling relation is changed to $\sigma_{AHE} \sim \sigma_{xx}^{1.6}$, indicating a crossover of the dominant contribution to σ_{AHE}, from the intrinsic Berry phase to the impurity scatterings. Our results show the intrinsic contribution from Berry curvature plays a crucial role in the anomalous Hall effect in $NiCo_2O_4$ films.

DOI: 10.1103/PhysRevB.104.134407

I. INTRODUCTION

The anomalous Hall effect is one of the best-explored magnetotransport properties of magnetic materials and their artificial heterostructures and has been widely exploited as a powerful probe of emergent magnetism and topological phases. The intrinsic anomalous Hall conductivity $\sigma_{AHE} = \rho_{AHE}/(\rho_{xx}^2 + \rho_{AHE}^2)$ (ρ_{xx}: longitudinal electrical resistivity, ρ_{AHE}: anomalous Hall resistivity) is closely tied with the Berry curvature originating from band structures and with scatterings of conduction electrons through spin-orbit interactions [1–5]. Electronic structures and electron scatterings (related to ρ_{xx} or the longitudinal electrical conductivity σ_{xx}) in magnetic heterostructures strongly depend on the thickness and dimension of constituent materials. It is, therefore, interesting to see how σ_{AHE}, σ_{xx}, and their correlations vary against thickness changes in magnetic materials.

The inverse-spinel $NiCo_2O_4$ (NCO) is a ferrimagnetic metal with a transition temperature above 400 K and a saturated magnetization of 1.5–2 μ_B per formula unit [6–9]. Epitaxial thin films of NCO on $MgAl_2O_4$ (MAO) substrates are found to have perpendicular magnetic anisotropy whose anisotropy energy is $0.1 \sim 0.2\,MJ/m^3$ at room temperature [10–14]. Theoretical investigations [15–18] show that NCO has the half-metallic band structure in which the density of states at the Fermi level E_F consists of only the minority-spin subband, and that the majority-spin one has a half-metallic energy gap at the E_F. The half-metallic nature in NCO has been supported by experimental observations of a large tunnel magnetoresistance effect (∼230%) in magnetic tunnel junctions based on NCO electrodes [19]. Calculated band structures also suggest that there are band crossings around E_F, which possibly act as either source or a sink of Berry curvature and are often manifested in magnetotransport properties such as anomalous Hall effect (AHE). Although the AHE is extensively used for evaluating spintronic properties, for example, perpendicular magnetic anisotropy [10,20], the AHE itself has not been explored in detail. In fact, recent magnetotransport characterizations of NCO epitaxial films have revealed temperature/thickness-induced sign reversal of AHE [12] and topological Hall-effect-like anomalies [21], which cannot be explained by the conventional framework of AHE where AHE is assumed to be proportional to the out-of-plane component of the magnetization.

In this study, we evaluated magnetotransport properties for epitaxial thin films of $NiCo_2O_4$ (NCO) whose thickness ranges from 3 to 30 nm. In contrast to previous reports [12,21], the sign of the anomalous Hall effect in all films evaluated in this study is found to be always negative, and no sign reversal is seen. The anomalous Hall resistivity ρ_{AHE} undergoes nonmonotonic changes with the temperature while the magnetization changes monotonically. This ρ_{AHE}'s behavior cannot be explained by the conventional framework of AHE. We also find that the anomalous Hall conductivity σ_{AHE} of the NCO films has rather complex relations with the longitudinal conductivity σ_{xx} in which the scaling relation between σ_{AHE} and σ_{xx} changes with increasing σ_{xx}. Our observations imply the significant contribution of Berry curvature to the anomalous Hall effect in NCO.

II. EXPERIMENTAL DETAILS

NCO films (from 3 to 30 nm thick) were epitaxially grown on (100) $MgAl_2O_4$ substrates by pulsed laser deposition. Details of NCO film growth were provided in our previous studies [10,11]. Briefly, NCO films were deposited at the substrate temperature of 315°C and under an oxygen partial pressure of 100 mTorr. It is noted that for NCO film grown by pulsed laser deposition, cation distribution strongly depends on the oxygen pressure during NCO deposition, and all films investigated in this study were grown under the optimized growth conditions that can produce NCO epitaxial

*dkan@scl.kyoto-u.ac.jp

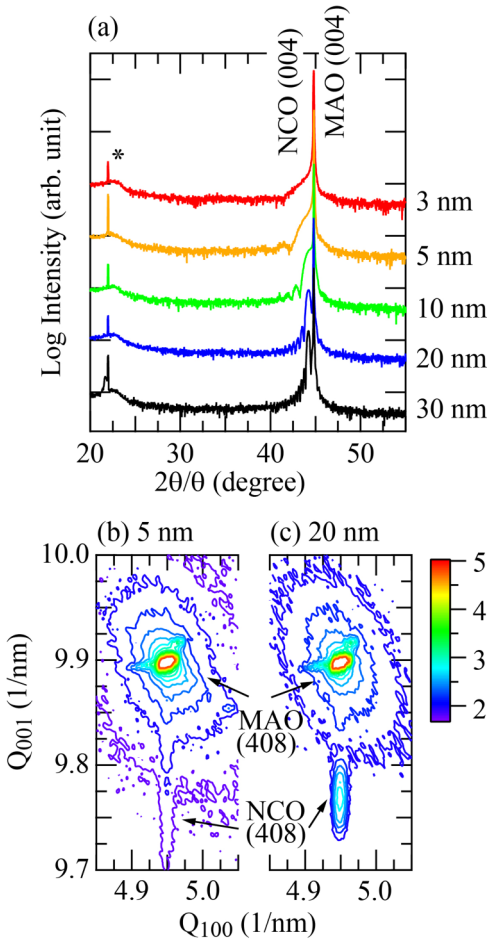

FIG. 1. X-ray $2\theta/\theta$ diffraction profiles around (004) $MgAl_2O_4$ (MAO) substrates for NCO epitaxial films whose thickness ranges from 3 to 30 nm. The peaks marked with the asterisk (*) probably originate from multiple scatterings from the MAO substrates. (b), (c) Reciprocal-space mappings around the (408) MAO reflection for (b) 5-nm-thick and (c) 20-nm-thick films. The intensity of the (408) NCO reflection for the 3-nm-thick film was too weak to be detected with our laboratory-source x-ray diffractometer.

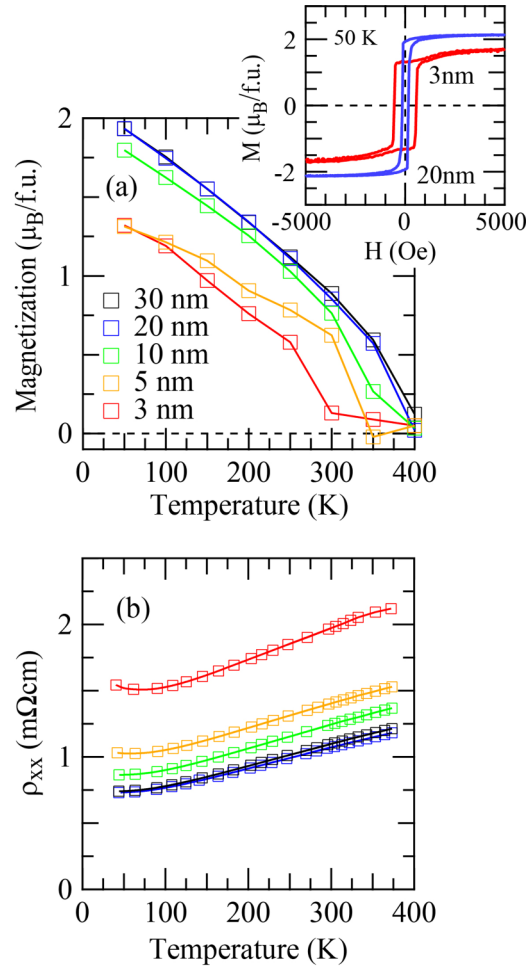

FIG. 2. (a) Temperature dependence of the magnetization of the NCO epitaxial films. The magnetization was determined as the remnant magnetization value extracted from the out-of-plane *M-H* curves, as shown in the inset. The M-H loops presented in the inset were taken at 50 K. (b) Temperature dependence of the longitudinal electrical resistivity ρ_{xx} for NCO epitaxial films.

films whose cation distribution is close to the stoichiometric [10]. The thickness of grown films was determined from the periods of the interference fringes seen in the x-ray $2\theta/\theta$ diffraction and reflectivity profiles.

III. RESULTS AND DISCUSSION

Figure 1 shows typical $2\theta/\theta$ diffraction profiles and reciprocal-space mappings for NCO films. The $2\theta/\theta$ profiles confirm that the NCO films are epitaxially grown with the (001) orientation and that no secondary phases are confirmed from the $2\theta/\theta$ pattern. Furthermore, the reciprocal-space mappings show that in-plane lattices of the films are fixed by those of the substrate and that the NCO layers are coherently grown on the substrate. We note that these structural properties are seen for all the films with thicknesses up to 30 nm.

Figure 2(a) shows the temperature dependence of the remnant magnetization of the NCO films. The remnant magnetization was determined from the out-of-plane magnetic field dependence of the magnetization, as shown in the inset of the figure. In each *M-H* loop, diamagnetic signals from the substrates were extracted by linearly fitting the data in larger field regions and were subtracted from measured data. We see that almost square-shaped hysteresis is seen in the out-of-plane *M-H* loops at temperatures below the ferrimagnetic transition temperature, even for the 3-nm-thick films. Note that *M-H* loops essentially the same as those in the inset are seen for all the films investigated in this study, consistent with the fact that our NCO films have perpendicular magnetic anisotropy. The magnetization increases monotonically with decreasing temperature regardless of the film thickness. When the film thickness is reduced, the magnetization is smaller.

To characterize magnetotransport properties of NCO films, we patterned the film layer to 15-μm-wide Hall bars by conventional photolithography and Ar-ion milling. We measured the longitudinal and transverse resistivities (ρ_{xx} and ρ_{xy}) by applying direct currents along the bars. Figure 2(b) shows the temperature dependence of ρ_{xx} of the NCO films. All films exhibit metallic electrical conduction down to low tem-

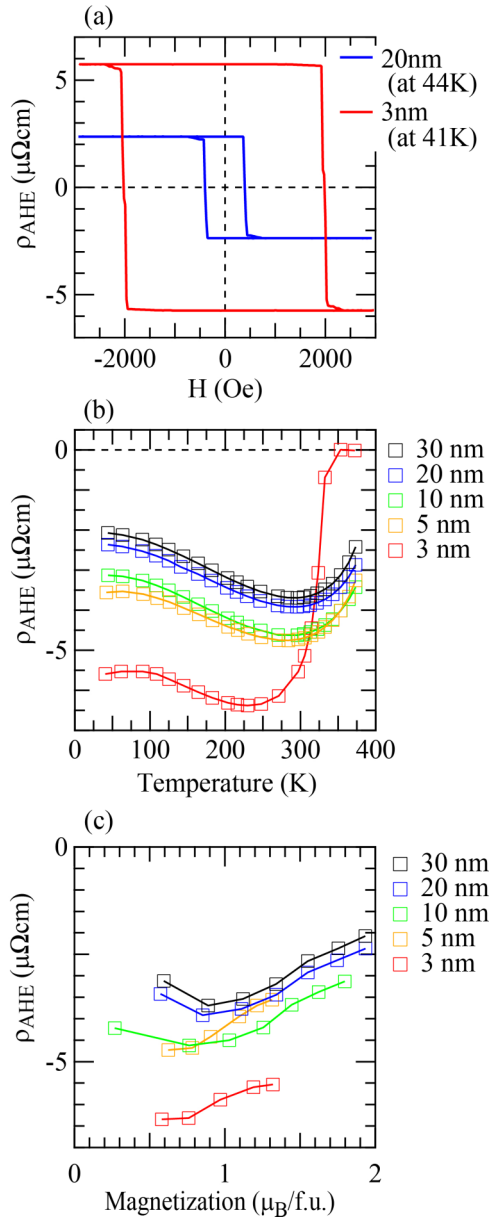

FIG. 3. (a) Typical magnetic field dependence of the anomalous Hall resistivity ρ_{AHE} for the 20-nm-thick (blue) and 3-nm-thick (red) NCO films. The magnetic fields were swept at a rate of 5 Oe/s. (b) Temperature dependence of the remnant ρ_{AHE} for NCO films. The remnant ρ_{AHE} was extracted from ρ_{AHE}-H curves as shown in (a). (c) ρ_{AHE} plotted against the magnetization of NCO films.

peratures, although the ρ_{xx} is larger for the thinner films. In addition, the thinner films exhibit larger upturns in the ρ_{xx} at low temperatures. Previously it was shown that the ρ_{xx}'s upturn at low temperatures is caused by disorders and defects related to deviations of the cation occupations from the stoichiometric [10]. Our observation of the upturn behavior enhanced for the thinner films implies that the influence of disorder scatterings of the conduction electrons on transport properties becomes dominant when the film thickness is reduced to a few nanometers.

Figure 3(a) shows the magnetic field dependence of the anomalous Hall resistivity ρ_{AHE} for the 20- and 3-nm-thick films measured at 50 K. The ρ_{AHE} was extracted as follows. We first antisymmetrized the ρ_{xy} so that asymmetric components included in the ρ_{xy} that resulted from misalignments of samples are corrected. We then determined the ordinary part of the Hall resistivity by linearly fitting the antisymmetrized ρ_{xy} in the higher magnetic field region. Finally, the ρ_{AHE} was extracted by subtracting the ordinary Hall resistivity from the antisymmetrized ρ_{xy}. For both films, the sign of the ρ_{AHE} is negative, and the square-shaped hysteresis with the remnant ρ_{AHE} comparable to the saturated one is seen. These behaviors of the ρ_{AHE} are characteristic of perpendicularly magnetized films. Note that ρ_{AHE}-H loops essentially the same as those in Fig. 3(a) are seen regardless of the film thickness. Figure 3(b) shows the temperature dependence of the remnant ρ_{AHE} for the NCO films. The ρ_{AHE} is negative throughout the temperature region investigated here and changes nonmonotonically with the temperature. The ρ_{AHE} of the 3-nm-thick film is greatly reduced above 300 K and becomes almost zero at ∼370 K. These observations imply that the NCO's ferrimagnetic transition temperature is lowered when the film thickness is reduced to a few nanometers.

With decreasing temperature below the ferrimagnetic transition temperature, the ρ_{AHE} begins to develop and shows the maximum in its magnitude at a specific temperature (which we call T_S). Below T_S, the ρ_{AHE}'s magnitude gradually decreases. For the 3- and 5-nm-thick films, slight increases in the ρ_{AHE}'s magnitude are also seen at low temperatures. Interestingly, the temperature at which the ρ_{AHE}'s magnitude slightly increases coincides with the temperature at which the upturn behavior of the ρ_{xx} is seen. This correlation between ρ_{AHE} and ρ_{xx} implies that the ρ_{AHE} varies with ρ_{xx}. It is also worthwhile pointing out that the ρ_{AHE}'s magnitude is larger when the magnetization is smaller, as shown in Fig. 3(c) where the ρ_{AHE} is plotted as a function of the magnetization. Furthermore, the ρ_{AHE} changes nonmonotonically with the temperature, while the magnetization changes monotonically. These observations indicate that the ρ_{AHE} depends on the magnetization in a complicated manner, not linearly as expected from the conventional framework of the anomalous Hall effect. It can thus be concluded that the Berry curvature plays a significant role in the behavior of the negative ρ_{AHE} of NCO films, especially at temperatures below T_S. It is worth pointing out that, in contrast to previous reports [12,21], neither sign reversal nor anomalies in ρ_{AHE} such as hump structures in ρ_{AHE}-H loops are seen for our films. Given that the intrinsic Berry curvature leads to the negative AHE, the previously observed sign reversal in ρ_{AHE} implies the coexistence of additional positive AHE. Because cation distribution in NCO films depends on growth conditions and often deviates from the stoichiometric one, positive AHE probably originates from some defects related to deviations of cation distribution. This is also consistent with our observation of no sign reversal for our films whose cation distribution is close to the stoichiometric. Such defects would also lead to inhomogeneities in coercive fields (Hc), leading to topological Hall-effect-like anomalies [22].

To further explore scaling relations of the anomalous Hall effect in NCO films, we focused on the anomalous Hall conductivity $\sigma_{AHE} = \rho_{AHE}/(\rho_{xx}^2 + \rho_{AHE}^2)$, which is known to exhibit the power-law dependence on the σ_{xx} in various ways depending on material properties. According to

quantum transport theory for multiband magnetic metals [1,2,23–25], the σ_{AHE} is intrinsically proportional to the integral of the Berry curvature over the filled electronic states. This intrinsic σ_{AHE} is insensitive to impurity scattering and is thus independent of σ_{xx} (or the scattering rate). On the other hand, for materials with low σ_{xx} ($<10^3 \sim 10^4\ \Omega^{-1}\ cm^{-1}$), in which the (impurity) scattering rate is increased, the intrinsic contribution is damped, and the scaling $\sigma_{AHE} \sim \sigma_{xx}^{1.6}$ is seen [26–29]. Given that the σ_{xx} of the NCO is about $10^3\ \Omega^{-1}\ cm^{-1}$ [Fig. 2(b)], the σ_{AHE} would follow different scaling relations depending on the magnitude of σ_{xx}. When the σ_{xx} is smaller, the scaling relation of $\sigma_{AHE} \sim \sigma_{xx}^{1.6}$ would be expected. On the other hand, the σ_{AHE} would become constant independent of σ_{xx} when the σ_{xx} becomes larger.

Figure 4(a) shows the σ_{xx} dependence of σ_{AHE}. For clarity, the line representing the $\sigma_{AHE} \sim \sigma_{xx}^{1.6}$ scaling relation is also shown. Interestingly, the σ_{AHE} below T_S (in the region of σ_{xx} larger than the arrowed data) for different NCO films with various thicknesses follows the single trend against the σ_{xx}'s variations. When σ_{xx} is lower than $10^3\ \Omega^{-1}\ cm^{-1}$, the σ_{AHE} follows the scaling relation $\sigma_{AHE} \sim \sigma_{xx}^{1.6}$. On the other hand, when σ_{xx} is larger than $10^3\ \Omega^{-1}\ cm^{-1}$, the σ_{AHE} becomes almost independent of the σ_{xx}, deviating from the $\sigma_{AHE} \sim \sigma_{xx}^{1.6}$ line. This σ_{AHE}'s behavior indicates that the intrinsic Berry curvature of the occupied electronic states is the key for the σ_{AHE} in the region of σ_{xx} larger than $10^3\ \Omega^{-1}\ cm^{-1}$. When the σ_{xx} is lowered (for thinner films), the intrinsic contribution is damped due to the increased scattering rate, leading to the σ_{xx}-dependent crossover to the σ_{AHE}'s scaling relation of $\sigma_{AHE} \sim \sigma_{xx}^{1.6}$ [Fig. 4(a)]. While relationships between σ_{AHE} and σ_{xx} in NCO films have been investigated, the σ_{xx}-independent σ_{AHE} (in the larger σ_{xx} region) and the σ_{xx}-dependent crossover of the σ_{AHE}'s scaling relation have not been observed so far [12].

We also show that the σ_{AHE}'s magnitude increases monotonically with decreasing temperature, as shown in Fig. 4(b), and it becomes smaller for thinner films. These temperature- and thickness dependences of σ_{AHE} are very similar to those of the magnetization. An important implication of this observation is that the σ_{AHE} has a scaling relation with the magnetization, which contrasts with the ρ_{AHE}'s behavior (Fig. 3). In Fig. 4(c), the σ_{AHE} at temperatures below T_S is plotted against the magnetization. We see the scaling relation between the σ_{AHE} and the magnetization, especially for the σ_{AHE} that is of the intrinsic origin and almost independent of the σ_{xx} (mainly for the films thicker than 10 nm). A similar scaling relation between the σ_{AHE} and magnetization was reported for the itinerant ferromagnet $SrRuO_3$ in which Berry curvature is manifested in magnetotransport properties [30–32]. The σ_{AHE}'s scaling behavior with the magnetization for NCO films implies that the σ_{AHE} is sensitive to variations in electron distribution and exchange splitting associated with magnetization changes, highlighting the significance of the Berry curvature (or band crossings around E_F) on the anomalous Hall effect in NCO epitaxial films.

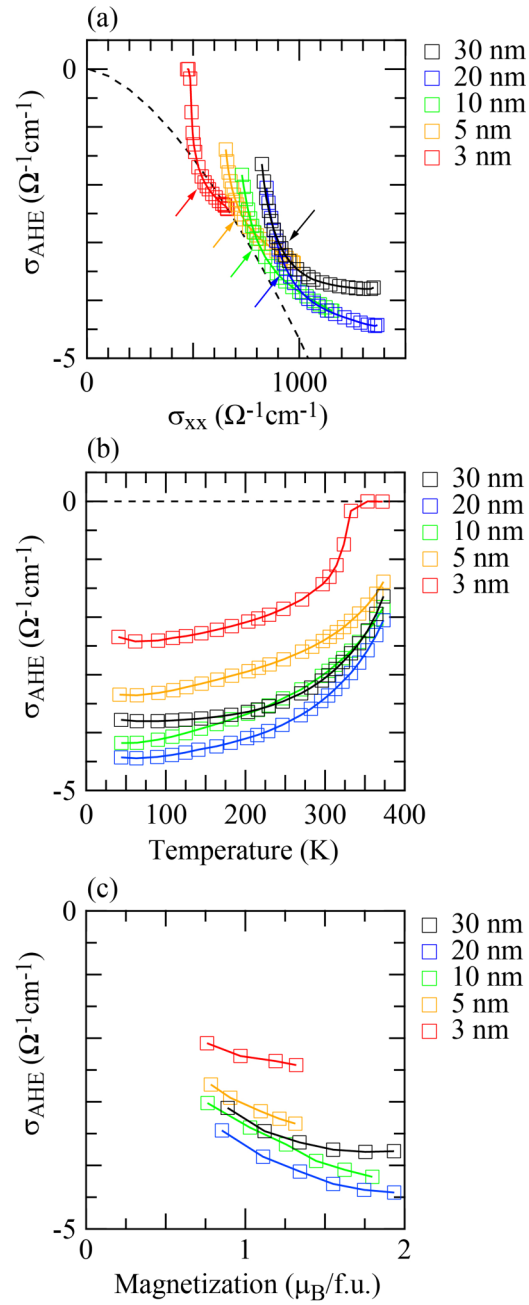

FIG. 4. (a) Anomalous Hall conductivity σ_{AHE} plotted against longitudinal electrical conductivity ρ_{xx} for NCO films. The data indicated with the arrows correspond to the σ_{AHE} at T_S. The black dotted line represents the scaling relation $\sigma_{AHE} \sim \sigma_{xx}^{1.6}$. (b) Temperature dependence of σ_{AHE} for NCO films. (c) σ_{AHE} plotted against the magnetization in the temperature region below T_S.

IV. SUMMARY

We investigate the anomalous Hall effect for perpendicularly magnetized $NiCo_2O_4$ epitaxial thin films with various thicknesses up to 30 nm. We find that the anomalous Hall conductivity σ_{AHE} is almost independent of the longitudinal conductivity σ_{xx} when the σ_{xx} is relatively large (larger than $10^3\ \Omega^{-1}\ cm^{-1}$). This σ_{AHE}'s behavior indicates that the intrinsic contribution of Berry curvature is a key for the AHE in NCO films. This intrinsic nature of AHE was further confirmed from the scaling behavior between the σ_{AHE} and the magnetization. We also show that with lowering σ_{xx}, the scaling relation is changed to $\sigma_{AHE} \sim \sigma_{xx}^{1.6}$, indicating a crossover

of the dominant contribution to σ_{AHE}, from the intrinsic Berry phase to the impurity scatterings.

ACKNOWLEDGMENTS

This work was partly supported by Grants-in-Aid for Scientific Research (Grants No. 19H05816, No. 19H05823, and No. 21H01810) and by grants for the Integrated Research Consortium on Chemical Sciences and the International Collaborative Research Program of Institute for Chemical Research in Kyoto University from the Ministry of Education, Culture, Sports, Science and Technology (MEXT) of Japan. This work was also supported by the Japan Society for the Promotion of Science Core-to-Core Program (A) Advanced Research Networks.

[1] N. Nagaosa, J. Sinova, S. Onoda, A. H. MacDonald, and N. P. Ong, Rev. Mod. Phys. **82**, 1539 (2010).
[2] T. Jungwirth, Q. Niu, and A. H. MacDonald, Phys. Rev. Lett. **88**, 207208 (2002).
[3] Y. Yao, L. Kleinman, A. H. MacDonald, J. Sinova, T. Jungwirth, D.-S. Wang, E. Wang, and Q. Niu, Phys. Rev. Lett. **92**, 037204 (2004).
[4] J. Ye, Y. B. Kim, A. J. Millis, B. I. Shraiman, P. Majumdar, and Z. Tešanović, Phys. Rev. Lett. **83**, 3737 (1999).
[5] Y. Taguchi, Y. Oohara, H. Yoshizawa, N. Nagaosa, and Y. Tokura, Science **291**, 2573 (2001).
[6] P. D. Battle, A. K. Cheetham, and J. B. Goodenough, Mater. Res. Bull. **14**, 1013 (1979).
[7] J. F. Marco, J. R. Gancedo, M. Gracia, J. L. Gautier, E. Ríos, and F. J. Berry, J. Solid State Chem. **153**, 74 (2000).
[8] J. F. Marco, J. R. Gancedo, M. Gracia, J. L. Gautier, E. I. Ríos, H. M. Palmer, C. Greaves, and F. J. Berry, J. Mater. Chem. **11**, 3087 (2001).
[9] D. Pyke, K. K. Mallick, R. Reynolds, and A. K. Bhattacharya, J. Mater. Chem. **8**, 1095 (1998).
[10] Y. Shen, D. Kan, Z. Tan, Y. Wakabayashi, and Y. Shimakawa, Phys. Rev. B **101**, 094412 (2020).
[11] D. Kan, I. Suzuki, and Y. Shimakawa, Jpn. J. Appl. Phys. **59**, 110905 (2020).
[12] X. Chen, X. Zhang, M.-G. Han, L. Zhang, Y. Zhu, X. Xu, and X. Hong, Adv. Mater. **31**, 1805260 (2019).
[13] Y. Bitla, Y.-Y. Chin, J.-C. Lin, C. N. Van, R. Liu, Y. Zhu, H.-J. Liu, Q. Zhan, H.-J. Lin, C.-T. Chen, Y.-H. Chu, and Q. He, Sci. Rep. **5**, 15201 (2015).
[14] C. Mellinger, J. Waybright, X. Zhang, C. Schmidt, and X. Xu, Phys. Rev. B **101**, 014413 (2020).
[15] P. F. Ndione, Y. Shi, V. Stevanovic, S. Lany, A. Zakutayev, P. A. Parilla, J. D. Perkins, J. J. Berry, D. S. Ginley, and M. F. Toney, Adv. Funct. Mater. **24**, 610 (2014).
[16] M. Wang, X. Sui, Y. Wang, Y.-H. Juan, Y. Lyu, H. Peng, T. Huang, S. Shen, C. Guo, J. Zhang, Z. Li, H.-B. Li, N. Lu, A. T. N'Diaye, E. Arenholz, S. Zhou, Q. He, Y.-H. Chu, W. Duan, and P. Yu, Adv. Mater. **31**, 1900458 (2019).
[17] R. Zhang, M. Liu, W. Liu, and H. Wang, Mater. Lett. **199**, 164 (2017).
[18] X. Shi, S. L. Bernasek, and A. Selloni, J. Phys. Chem. C **120**, 14892 (2016).
[19] Y. Shen, D. Kan, I.-C. Lin, M.-W. Chu, I. Suzuki, and Y. Shimakawa, Appl. Phys. Lett. **117**, 042408 (2020).
[20] D. Kan, I. Suzuki, and Y. Shimakawa, J. Appl. Phys. **129**, 183902 (2021).
[21] C. Wu, W. Guo, C. Zhen, H. Wang, G. Li, L. Ma, and D. Hou, J. Appl. Phys. **126**, 043901 (2019).
[22] D. Kan, T. Moriyama, K. Kobayashi, and Y. Shimakawa, Phys. Rev. B **98**, 180408(R) (2018).
[23] M. Onoda and N. Nagaosa, J. Phys. Soc. Jpn. **71**, 19 (2002).
[24] S. Onoda, N. Sugimoto, and N. Nagaosa, Phys. Rev. Lett. **97**, 126602 (2006).
[25] A. A. Kovalev, J. Sinova, and Y. Tserkovnyak, Phys. Rev. Lett. **105**, 036601 (2010).
[26] T. Fukumura, H. Toyosaki, K. Ueno, M. Nakano, T. Yamasaki, and M. Kawasaki, Jpn. J. Appl. Phys. **46**, L642 (2007).
[27] D. Venkateshvaran, W. Kaiser, A. Boger, M. Althammer, M. S. Ramachandra Rao, S. T. B. Goennenwein, M. Opel, and R. Gross, Phys. Rev. B **78**, 092405 (2008).
[28] T. Miyasato, N. Abe, T. Fujii, A. Asamitsu, S. Onoda, Y. Onose, N. Nagaosa, and Y. Tokura, Phys. Rev. Lett. **99**, 086602 (2007).
[29] W. R. Branford, K. A. Yates, E. Barkhoudarov, J. D. Moore, K. Morrison, F. Magnus, Y. Miyoshi, P. M. Sousa, O. Conde, A. J. Silvestre, and L. F. Cohen, Phys. Rev. Lett. **102**, 227201 (2009).
[30] Z. Fang, N. Nagaosa, K. S. Takahashi, A. Asamitsu, R. Mathieu, T. Ogasawara, H. Yamada, M. Kawasaki, Y. Tokura, and K. Terakura, Science **302**, 92 (2003).
[31] R. Mathieu, A. Asamitsu, H. Yamada, K. S. Takahashi, M. Kawasaki, Z. Fang, N. Nagaosa, and Y. Tokura, Phys. Rev. Lett. **93**, 016602 (2004).
[32] J. Matsuno, N. Ogawa, K. Yasuda, F. Kagawa, W. Koshibae, N. Nagaosa, Y. Tokura, and M. Kawasaki, Sci. Adv. **2**, e1600304 (2016).